

Sixty-Four Curves of Degree Six

Nidhi Kaihnsa, Mario Kummer, Daniel Plaumann,
Mahsa Sayyary Namin, and Bernd Sturmfels

Abstract

We present a computational study of smooth curves of degree six in the real projective plane. In the Rokhlin–Nikulin classification, there are 56 topological types, refined into 64 rigid isotopy classes. We developed software that determines the topological type of a given sextic and used it to compute empirical probability distributions on the various types. We list 64 explicit representatives with integer coefficients, and we perturb these to draw many samples from each class. This allows us to explore how many of the bitangents, inflection points and tensor eigenvectors are real. We also study the real tensor rank, the construction of quartic surfaces with prescribed topology, and the avoidance locus, which is the locus of all real lines that do not meet a given sextic. This is a union of up to 46 convex regions, bounded by the dual curve.

1 Topology

A classical theme in real algebraic geometry is the topological classification of algebraic curves in the real projective plane $\mathbb{P}_{\mathbb{R}}^2$. Hilbert’s 16th problem asks for the *topological types* of smooth curves of a fixed degree d , where two curves C and C' have the same type if some homeomorphism of $\mathbb{P}_{\mathbb{R}}^2 \rightarrow \mathbb{P}_{\mathbb{R}}^2$ restricts to a homeomorphism $C_{\mathbb{R}} \rightarrow C'_{\mathbb{R}}$. A finer notion of equivalence comes from the *discriminant* Δ . This is an irreducible hypersurface of degree $3(d-1)^2$ in the projective space $\mathbb{P}_{\mathbb{R}}^{d(d+3)/2}$ of curves of degree d . Points on Δ are singular curves. The *rigid isotopy classes* are the connected components of the complement $\mathbb{P}_{\mathbb{R}}^{d(d+3)/2} \setminus \Delta$. If two curves C and C' are in the same rigid isotopy class, then they have the same topological type, but the converse is not true in general, as shown by Kharlamov [20].

Hilbert’s 16th problem has been solved up to $d = 7$, thanks to contributions by many mathematicians, including Hilbert [17], Rohn [31], Petrovsky [29], Rokhlin [32], Gudkov [16], Nikulin [28], Kharlamov [20], and Viro [37, 38, 39]. In this article we focus on the case $d = 6$. Our point of departure is the following well-known classification of sextics, found in [38, §7].

Theorem 1.1 (Rokhlin–Nikulin). *The discriminant of plane sextics is a hypersurface of degree 75 in $\mathbb{P}_{\mathbb{R}}^{27}$ whose complement has 64 connected components. The 64 rigid isotopy types are grouped into 56 topological types, with the number of ovals ranging from 0 to 11. The distribution is shown in Table 1. The 56 types form the partially ordered set in Figure 1.*

Number of ovals	0	1	2	3	4	5	6	7	8	9	10	11	total
Count of rigid isotopy types	1	1	2	4	4	7	6	10	8	12	6	3	64
Count of topological types	1	1	2	4	4	5	6	7	8	9	6	3	56

Table 1: Rokhlin–Nikulin classification of smooth sextics in the real projective plane

The 64 types in Theorem 1.1 were known to Rokhlin [32]. The classification was completed by Nikulin. It first appeared in his paper [28] on the arithmetic of real K3 surfaces.

Every connected component C_0 of a smooth curve C in $\mathbb{P}_{\mathbb{R}}^2$ is homeomorphic to a circle. If the complement $\mathbb{P}_{\mathbb{R}}^2 \setminus C_0$ is disconnected, then C_0 is called an *oval*, otherwise a *pseudoline*. If C has even degree, then all connected components are ovals. A curve of odd degree has exactly one pseudoline. The two connected components of the complement of an oval are called the *inside* and the *outside*. The former is homeomorphic to a disk, the latter to a Möbius strip. An oval C_0 *contains* another oval C_1 if C_1 lies in the inside of C_0 . In that case, C_0 and C_1 are *nested ovals*. An oval is *empty* if it contains no other oval. The topological type of the curve C is determined by the number of ovals together with the information of how these ovals contain each other. We denote the type of a smooth plane sextic C in $\mathbb{P}_{\mathbb{R}}^2$ by

- k if C consists of k empty ovals;
- $(k1)l$ if C consists of an oval C_0 containing k empty ovals and of l further empty ovals lying outside C_0 ;
- (hyp) if C consists of three nested ovals (where 'hyp' stands for 'hyperbolic').

Figure 1 is a refinement of Viro's diagram in [39, Figure 4]. The top row contains the three types with 11 ovals. These are denoted (91)1, (51)5 and (11)9. The cover relations correspond to either fusing two ovals or shrinking an oval until it vanishes (cf. Theorem 4.4). We know from [28, p. 107] that all but eight of the 56 topological types correspond to exactly one rigid isotopy class, while the following eight types consist of two rigid isotopy classes:

$$(41) \quad (21)2 \quad (51)1 \quad (31)3 \quad (11)5 \quad (81) \quad (41)4 \quad 9. \quad (1)$$

For an irreducible curve C in $\mathbb{P}_{\mathbb{R}}^2$, the set $C_{\mathbb{C}} \setminus C_{\mathbb{R}}$ of non-real points in the Riemann surface has either one or two connected components. In the latter case we say that C is *dividing*.

The rigid isotopy type of a smooth plane sextic determines whether it is dividing or not. More precisely, the subset of $\mathbb{P}_{\mathbb{R}}^{27}$ consisting of all dividing sextics is the closure of the union of 14 rigid isotopy types. First, there are the eight topological types in (1). These can be dividing or not, by [28, Remark 3.10.10]. This explains the difference between the second row and third row of the table in Theorem 1.1. In addition, there are six topological types that are necessarily dividing. These are precisely the maximal elements in the poset of sextics:

$$(91)1 \quad (51)5 \quad (11)9 \quad (61)2 \quad (21)6 \quad (\text{hyp}). \quad (2)$$

In summary, of the 56 topological types of smooth plane sextics, precisely 42 types are non-dividing. The six types in (2) are dividing, and the eight types in (1) can be dividing

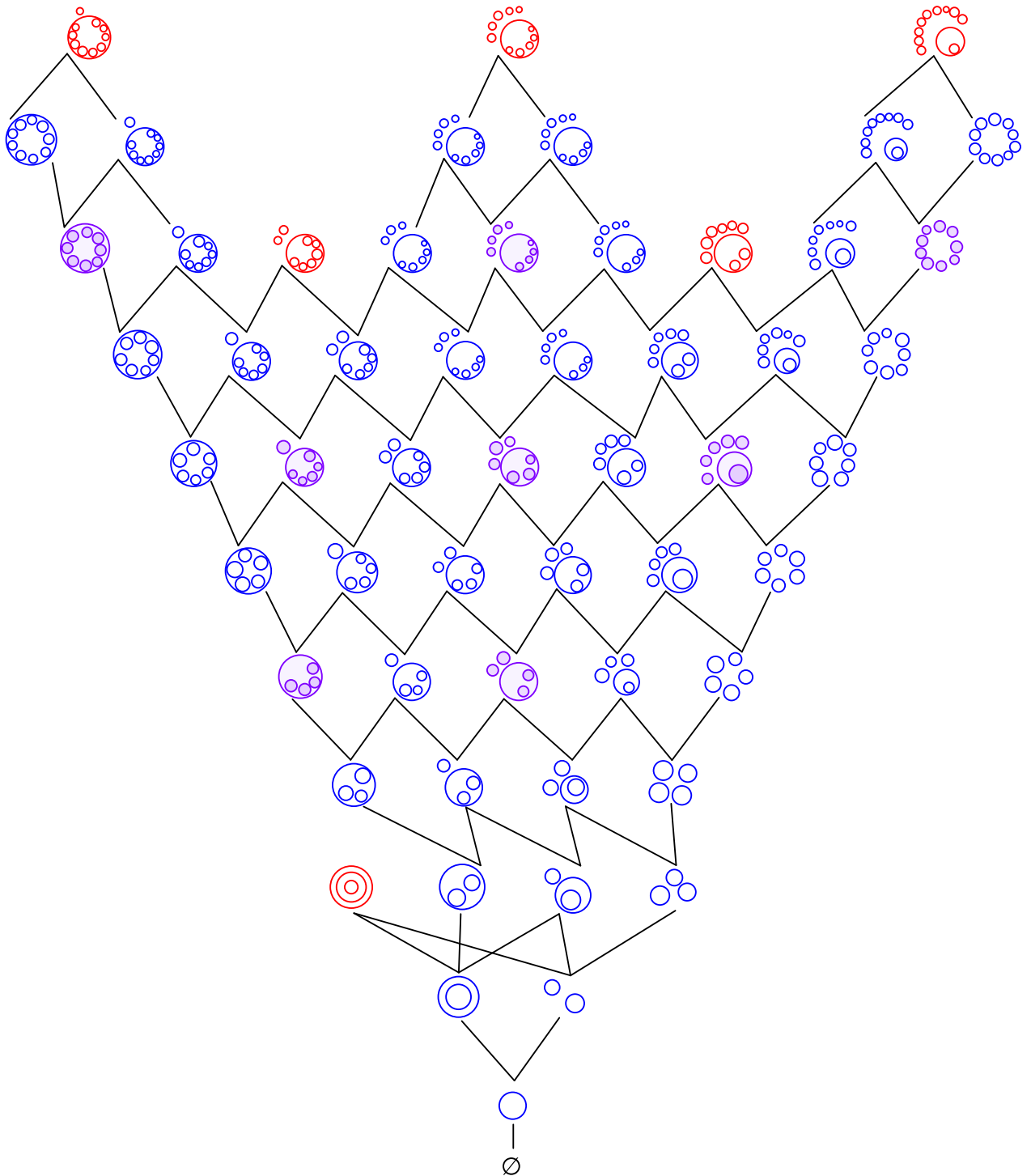


Figure 1: The 56 types of smooth plane sextics form a partially ordered set. The color code indicates whether the real curve divides its Riemann surface. The red curves are dividing, the blue curves are non-dividing, and the purple curves can be either dividing or non-dividing.

or non-dividing. Hence, there are 14 rigid isotopy types that are dividing. This accounts for all 64 rigid isotopy types (connected components of $\mathbb{P}_{\mathbb{R}}^{27} \setminus \Delta$) in the census of Theorem 1.1.

This paper presents an experimental study of the objects above, conducted with a view towards Applied Algebraic Geometry. Numerous emerging applications, notably in the analysis of data from the life sciences, now rely on computational tools from topology and algebraic geometry. A long-term goal that motivated this project is the development of connections between such applications and existing knowledge on the topology of real algebraic varieties.

The ecosystem to be explored in this particular study is the 27-dimensional space of plane sextic curves. Our focus lies on experimentation and exact computation with ternary sextics over the integers. Thus, our model organisms are homogeneous polynomials in $\mathbb{Z}[x, y, z]_6$.

We now summarize the contributions of this paper. In Section 2 we present a list of 64 polynomials in $\mathbb{Z}[x, y, z]_6$ that serve as representatives for the 64 rigid isotopy types. In Section 3 we describe methods for classifying a given ternary sextic according to Theorem 1.1. To determine the topological type we wrote fast code in `Mathematica` based on the built-in tool for *cylindrical algebraic decomposition* (CAD, [4]). This is used to sample sextics from natural probability distributions on $\mathbb{R}[x, y, z]_6 \simeq \mathbb{R}^{28}$, so as to find the empirical distributions on the 56 topological types. Distinguishing between dividing and non-dividing types is harder. Our primary tool for this is Proposition 4.6. For an alternative approach see [19].

In Section 4 we present a method for computing the discriminant, and we discuss our derivation of the 64 polynomial representatives. Section 5 concerns the subdivision of the dual projective plane $(\mathbb{P}^2)_{\mathbb{R}}^{\vee}$ by a curve C^{\vee} of degree 30, namely that dual to a given sextic C . The nodes of C^{\vee} are the 324 bitangents of C . We study how many of them are real for each of the 64 types. These numbers do not depend on the topological or rigid isotopy type alone. They are reported in Table 7. Real lines that miss $C_{\mathbb{R}}$ form the avoidance locus \mathcal{A}_C . This is a union of up to 46 convex regions, bounded by the dual curve. In Section 6 we explore inflection points, tensor eigenvectors, real tensor rank, and connections to K3 surfaces.

Many new results and questions can be derived by the computational framework developed in this paper. Here is one example. It concerns reducible sextic curves consisting of six distinct lines. This 12-dimensional family in $\mathbb{P}_{\mathbb{R}}^{27}$ is the *Chow variety* of factorizable forms.

Proposition 1.2. *Configurations of six general lines appear in the closure of precisely 35 of the 64 rigid isotopy classes. These are the classes that meet the Chow variety in a generic point. These 35 classes are marked with an asterisk in Table 7, in the column on eigenvectors.*

2 Representatives

We shall derive the following result by furnishing explicit polynomial representatives.

Proposition 2.1. *Each of the 64 rigid isotopy types can be realized by a ternary sextic in $\mathbb{Z}[x, y, z]_6$ whose integer coefficients have absolute value less than 1.5×10^{38} .*

We list 64 polynomials with integer coefficients that represent the 64 rigid isotopy types of smooth sextic curves in $\mathbb{P}_{\mathbb{R}}^2$. This list is available in a computer-algebra-friendly format at

$$\text{http://personal-homepages.mis.mpg.de/kummer/sixtyfour.html} \quad (3)$$

Each of our sextics is labeled by its topological type and whether it is dividing (d) or non-dividing (nd) in its Riemann surface. We begin with the 35 types that have at most 7 ovals:

	0	nd	$x^6 + y^6 + z^6$
	1	nd	$x^6 + y^6 - z^6$
(11)	nd		$6(x^4 + y^4 - z^4)(x^2 + y^2 - 2z^2) + x^5y$
	2	nd	$(x^4 + y^4 - z^4)((x + 4z)^2 + (y + 4z)^2 - z^2) + z^6$
(21)	nd		$16((x+z)^2 + (y+z)^2 - z^2)(x^2 + y^2 - 7z^2)((x-z)^2 + (y-z)^2 - z^2) + x^3y^3$
(11)1	nd		$((x + 2z)^2 + (y + 2z)^2 - z^2)(x^2 + y^2 - 3z^2)(x^2 + y^2 - z^2) + x^5y$
	3	nd	$(x^2 + y^2 - z^2)(x^2 + y^2 - 2z^2)(x^2 + y^2 - 3z^2) + x^6$
(hyp)	d		$6(x^2 + y^2 - z^2)(x^2 + y^2 - 2z^2)(x^2 + y^2 - 3z^2) + x^3y^3$
(31)	nd		$(10(x^4 - x^3z + 2x^2y^2 + 3xy^2z + y^4) + z^4)(x^2 + y^2 - z^2) + x^5y$
(21)1	nd		$(10(x^4 - x^3z + 2x^2y^2 + 3xy^2z + y^4) + z^4)((x + z)^2 + y^2 - 2z^2) + x^5y$
(11)2	nd		$(10(x^4 - x^3z + 2x^2y^2 + 3xy^2z + y^4) + z^4)(x^2 + (y - z)^2 - z^2) + x^5y$
	4	nd	$x^6 + y^6 + z^6 - 4x^2y^2z^2$
(41)	nd		$((x^2 + 3y^2 - 20z^2)(4x^2 + y^2 - 16z^2) + 18x^2z^2)(x^2 + y^2 - 10z^2) - 2z^6$
(41)	d		$10(((x^2+2y^2-16z^2)(2x^2+y^2-16z^2) + x^2y^2)(10x + y + 5z) + xz^4)(10x - y - 8z) - xz^5$
(31)1	nd		$((x^2 + 3y^2 - 17z^2)(3x^2 + y^2 - 10z^2) + 15x^2z^2)(x^2 + 4(y + z)^2 - 25z^2) + x^3y^3$
(21)2	nd		$((x^2+3y^2-20z^2)(4x^2+y^2-16z^2) + 18x^2z^2)((x+y)^2 + 20(x-y-3z)^2 - 24z^2) + (y-x)z^5$
(21)2	d		$((x^2 + 3y^2 - 20z^2)(4x^2 + y^2 - 16z^2) + 18x^2z^2)(x^2 + 8y^2 - 16z^2) - 4z^6$
(11)3	nd		$((x^2 + 2y^2 - 30z^2)(3x^2 + y^2 - 20z^2) + 15x^2z^2)(x^2 + (4y + 16z)^2 - 15z^2) + x^3y^3$
	5	nd	$4((x^2 + 2y^2 - 4z^2)(2x^2 + y^2 - 4z^2) + z^4)(x^2 + y^2 - z^2) + x^3y^3$
(51)	nd		$(3x^2 + 4xy + 2y^2 - 4z^2)(x^2 + 2(y - z)^2 - 8z^2)(2x^2 + y^2 - 3z^2) - z^6$
(41)1	nd		$(4x^2 + 6x(y-z) + 3(y-z)^2 - 14z^2)(x^2 + 5(y-2z)^2 - 9z^2)(2x^2 + (y-z)^2 - 15z^2) - yz^5$
(31)2	nd		$((x+z)^2 + 4y^2 - 4z^2)(7(x+z)^2 + y^2 - 10z^2)((x+z)^2 + 4(2(x+y)+3z)^2 - 8z^2) + xz^5$
(21)3	nd		$((x+z)^2 + 3y^2 - 4z^2)(7(x+z)^2 + y^2 - 12z^2)((x+z)^2 + 3(2(x+y)+3z)^2 - 5z^2) + xz^5$
(11)4	nd		$((x^2 + 3y^2 - 20z^2)(4x^2 + y^2 - 16z^2) + 18x^2z^2)(8x^2 + y^2 - 16z^2) + (x+y)z^5$
	6	nd	$(3x^2 + 5xy + 2y^2 - 7z^2)(x^2 + 2(y - z)^2 - 8z^2)(2x^2 + y^2 - 5z^2) - z^6$
(61)	nd		$(4x^2 + 4xy + 3y^2 - 4z^2)(x^2 + 3y^2 - 4z^2)(4x^2 + y^2 - 4z^2) - z^6$
(51)1	nd		$30(((x-z)^2 + 3y^2 - 5z^2)(3(x-z)^2 + y^2 - 5z^2) + xz^3)((x-z)^2 + y^2 - 2z^2) + (x-2z)z^5$
(51)1	d		$7((x^2 + 3(y + z)^2 - 48z^2)(3(x + z)^2 + y^2 - 48z^2) - z^4)(x^2 + y^2 - 26z^2) + xz^5 + yz^5$
(41)2	nd		$15(4x^2 + y^2 - 3z^2)(x^2 + 3y^2 - 3z^2)((4x - z)^2 + 16y^2 - 22z^2) + (5xz^5 + (y - z)^3z^3)$
(31)3	nd		$34((3x^2 + y^2 - 3z^2)(x^2 + 8y^2 - 3z^2) + x^2y^2)(2x^2 - yz - 2z^2) + (x - 4z)yz^4$
(31)3	d		$((x^2 + 3y^2 - 28z^2)(4x^2 + y^2 - 20z^2) - z^4)((x + z)^2 + y^2 - 12z^2) - xz^5$
(21)4	nd		$27(2xz - 6y^2 + 2yz + 3z^2)(-(x + y)^2 - 4y^2 + 2z^2)(5(x + y)^2 + y^2 - 4z^2) - xz^5$
(11)5	nd		$((x^2 + 3y^2 - 20z^2)(4x^2 + y^2 - 16z^2) + 18x^2z^2)(16x^2 + y^2 - 20z^2) - (x + y)z^5$
(11)5	d		$((x^2+3y^2-20z^2)(4x^2+y^2-16z^2) + 18x^2z^2)((x+y)^2 + 20(x-y-3z)^2 - 24z^2) + (x+y)z^5$
	7	nd	$2(4x^2 + y^2 - 4z^2)(x^2 + 4y^2 - 5z^2)(x^2 + y^2 - 4z^2) + 3x^4y^2 + xy^5$

Next, we have eight topological types with eight ovals, all of which are non-dividing:

(71)	nd	$2(x^2 + y^2 - 26z^2)(x^2 + 3(y + z)^2 - 48z^2)(3(x + z)^2 + y^2 - 48z^2) - z^6$	
(21)5	nd	$40(3x^2 + y^2 - 3z^2)(x^2 + 8(y - z)^2 - 3z^2)(2x^2 - yz - 2z^2) - (y^3z^3 + 2xz^5 - 2z^6)$	
(11)6	nd	$19(4x^2 + y^2 - 4z^2)(x^2 + 8(y - z)^2 - 3z^2)(2x^2 - yz - 2z^2) - (2y - 3z)z^5$	
	8	nd	$12(x^4 + 2x^2y^2 + y^4 - x^3z + 3xy^2z)(7(8x + 3z)^2 + 8y^2 - 10z^2) + x^5y + 2z^6$

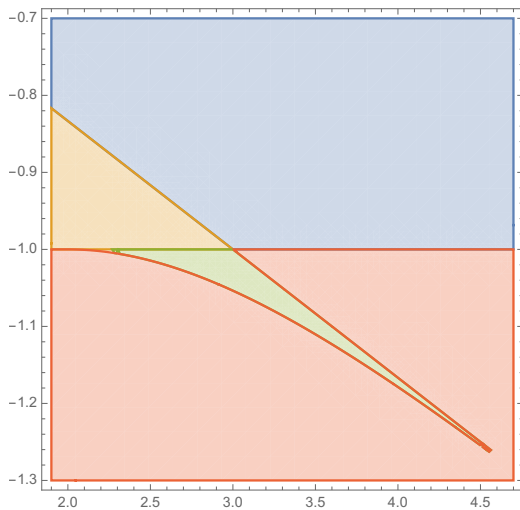


Figure 2: The discriminant divides the Robinson net (4) into 15 components that realize four topological types. The green region represents smooth sextics with 10 non-nested ovals.

where $(a : b : c)$ is any point in $\mathbb{P}_{\mathbb{R}}^2$. For $(a : b : c) = (19 : 60 : -20)$, this degree six curve is smooth and its real locus consists of ten non-nested ovals. This is a sextic we like, and we therefore included $\mathcal{R}(19, 60, -20)$ in the list above as our representative for the Type 10 nd.

We named this net of sextics after R.M. Robinson, who showed in 1973 that the special sextic $\mathcal{R}(1, 3, -1)$ is non-negative but is not a sum of squares. The reason is geometric: its real locus consists of 10 isolated singular points in $\mathbb{P}_{\mathbb{R}}^2$, given by the columns of the matrix

$$\begin{pmatrix} 1 & -1 & 1 & 1 & 0 & 0 & 1 & -1 & 1 & 1 \\ 1 & 1 & -1 & 1 & 1 & 1 & 0 & 0 & 1 & -1 \\ 1 & 1 & 1 & -1 & 1 & -1 & 1 & 1 & 0 & 0 \end{pmatrix}. \quad (5)$$

To understand how the topology of $\mathcal{R}(a, b, c)$ varies with $(a : b : c)$, we examine the complement of the discriminant in $\mathbb{P}_{\mathbb{R}}^2$. This is the following reducible polynomial of degree 75:

$$a^3(a+c)^6(3a-c)^{18}(3a+b+6c)^4(3a+b-3c)^8(9a^3-3a^2b+ab^2-3ac^2-bc^2+2c^3)^{12} \quad (6)$$

The complement of the discriminant in $\mathbb{P}_{\mathbb{R}}^2$ has 15 connected components. These realize the following topological types of smooth sextics: 10, 4, 3 and 0. These types are found in 1, 3, 5 and 6 connected components respectively. The most interesting part of the partition is shown in Figure 2. The green region is the component corresponding to curves with 10 ovals. Smooth curves in the orange, red and blue region have 0, 3 and 4 ovals respectively.

The Robinson net serves as a cartoon for the geometric object studied in this paper: the partition of a 27-dimensional real projective space into 64 connected components by an irreducible hypersurface of degree 75. Figure 2 is a two-dimensional slice of that partition.

3 Classifier and Empirical Distributions

Deriving the topology of a real plane curve from its equation is a well-studied problem in computational geometry. The main idea is to ascertain the topology of plane curves by constructing isotopic graphs whose nodes are the critical points (singular and extreme). Authors who studied this problem include Jinsan Cheng, Sylvain Lazard, Luis Peñaranda, Marc Pouget, Fabrice Rouillier, Elias Tsigaridas, Laureano González-Vega, Ioana Necula, M’hammed El Kahoui, Hoon Hong, Raimund Seidel, and Nicola Wolpert. See [8, 11, 15, 33].

The algorithm in [8] is called `ISOTOP`. It is implemented in `Maple` using certain packages written in `C`. We refer to [8, Table 1, page 28] for comparisons between `ISOTOP` and `Top`, as well as with `INSULATE`, `AlciX` [11], and `Cad2d` [4]. The latter two are implemented in `C++`.

After first experiments with these packages, we came to the conclusion that it is preferable for us to have our own specialized implementation for curves of degree six in $\mathbb{P}_{\mathbb{R}}^2$. In particular, all of the mentioned packages compute the topology of the curve in the affine chart $\{z = 1\}$. It was not obvious how to extract the topological type of the curve in the projective plane from the output with a reasonable amount of coding effort. Developers and users of the packages above may wish to experiment with our representatives for 10 and 11 ovals.

We wrote a program in `Mathematica` called `SexticClassifier`. It relies heavily on the built-in quantifier elimination techniques of `Mathematica`. The code can be obtained from our supplementary materials website (3). The input to `SexticClassifier` is a ternary sextic with integer coefficients, $f \in \mathbb{Z}[x, y, z]_6$. The code checks whether f defines a non-singular curve in $\mathbb{P}_{\mathbb{C}}^2$. If not, then the output is “singular”. Otherwise, our program identifies which of the 56 topological types the real curve $V_{\mathbb{R}}(f)$ belongs to. We next explain how it works.

First we compute a *Cylindrical Algebraic Decomposition* (CAD; see e.g. [3, 4]) of the curve $V_{\mathbb{R}}(f)$ in the affine chart $z = 1$. From this we build a graph whose nodes are the critical points of the projection along the y -axis. Two nodes are connected by an edge if an arc of the curve connects the corresponding points. We also keep track of the relative positions of these arcs. In order to get the correct topology in $\mathbb{P}_{\mathbb{R}}^2$, we add further edges corresponding to arcs crossing the line at infinity. We end up with a graph whose connected components are in one-to-one correspondence with the connected components of the curve. Finally, for each pair of connected components of the graph, we have to check whether one of the corresponding ovals lies in the inside of the other. This is done by first deciding whether the center of projection lies inside the ovals or not. Knowing this, detecting a nesting of two ovals only amounts to looking at the parity of the number of branches of one oval lying above the other oval. The program terminates correctly in less than four seconds for all sextics in Section 2. If the coefficients are between -10^8 and 10^8 , then it takes less than one second.

Example 3.1. Here is an instance that will be of interest in Section 5. Let f be the sextic

$$7(x + y + 2z)(x + 2y + z)(2x + y + z)(x - 2y + 3z)(y - 2z + 3x)(z - 2x + 3y) + xyz(x^3 + y^3 + z^3).$$

After checking that the complex curve $V_{\mathbb{C}}(f)$ is smooth, our code reveals that the real curve $V_{\mathbb{R}}(f)$ consists of three separate non-nested ovals. Thus, the input to `SexticClassifier` is the polynomial f and the output is the label 3. In particular, $V_{\mathbb{R}}(f)$ is non-dividing.

The sextic f has the property that every real line in \mathbb{P}^2 meets $V_{\mathbb{C}}(f)$ in at least one real point. Thus, $V_{\mathbb{R}}(f)$ is not compact in any affine chart of $\mathbb{P}_{\mathbb{R}}^2$, regardless of which line serves as the line at infinity. While such non-compact curves may cause difficulties in some of the approaches discussed above, `SexticClassifier` has been designed to handle them well. \diamond

Forty-eight of the fifty-six topological types determine whether the curve is dividing or not. However, the remaining eight were found by Nikulin [28] to split into two rigid isotopy types. Suppose that the output of `SexticClassifier` is one of the eight labels in (1). At present, we have no easy tool for deciding whether the given f is dividing or non-dividing. That decision requires us to build a model of the Riemann surface $V_{\mathbb{C}}(f)$ in order to ascertain whether $V_{\mathbb{C}}(f) \setminus V_{\mathbb{R}}(f)$ has one or two connected components. A method for making that decision was developed and implemented by Kalla and Klein [19], but presently their code is not suitable for curves of genus 10. One of our goals for the future is to extend `SexticClassifier` so that it decides rapidly between ‘d’ and ‘nd’ when the output is in (1).

As a first application of `SexticClassifier`, we computed the empirical distributions of the topological types over the space of ternary sextics. In other words, we ask: what is the probability that a particular topological type arises when we pick a sextic curve at random? Of course, the answer will depend on the choice of a probability distribution on the sextics

$$f = \sum_{i+j+k=6} c_{ijk} x^i y^j z^k. \quad (7)$$

A theoretical study for curves of large degree was carried out recently by Lerario and Lundberg [25], who employed the real Fubini-Study ensemble and the Kostlan distribution. Our experiments below are meant to inform this line of inquiry with some empirical numbers.

The first distribution we consider is $U(3)$ -invariant. The 28 coefficients c_{ijk} are chosen independently from a univariate normal distribution, centered at 0, with variance equal to the multinomial coefficient $6!/(i!j!k!)$. According to [7, §16.1], this is the unique $U(3)$ -invariant probability measure on $\mathbb{R}[x, y, z]_6$. We selected 1,500,000 samples, we ran `SexticClassifier` on these sextics, and we tallied the topological types. The result is shown in Table 2.

We see that the empirical distribution is very skewed. Only 14 of the 56 types were observed at all. Only six types had an empirical probability of $\geq 1\%$. No curve with more than six ovals was observed. In our sample, the average number of connected components is approximately 1.50. Another numerical invariant of the topological type of a smooth real plane curve introduced in [25, page 8] is the *energy*. This nonnegative integer measures the nesting of the ovals. For sextics, the maximal energy is 38 and attained by the Harnack-type curve (91)1. The average energy of the sextics in the sample above is approximately 2.99.

1	2	3	(11)	4	(11)1	(21)	5	\emptyset	(11)2	(21)1	6	(31)	(hyp)
875109	423099	97834	90316	7594	4360	1180	245	127	118	8	7	2	1

Table 2: Counts of topological types sampled from the $U(3)$ -invariant distribution

We experimented with several other distributions on $\mathbb{R}[x, y, z]_6$, each time drawing 500,000 samples and running `SexticClassifier`. In the following tables, we report percentages, and we only list topological types with empirical probability at least 0.01%.

1	2	3	(11)	\emptyset	4
77.52%	18.19%	2.11%	1.46%	0.66%	0.06%

Table 3: Sextics with coefficients in $\{-10^{12}, \dots, 10^{12}\}$ uniformly distributed

1	\emptyset	3	(11)	4	6	(31)	(11)3	7	(hyp)
45.69%	28.38%	16.15%	7.40%	2.17%	0.13%	0.03%	0.03%	0.01%	0.01%

Table 4: Symmetric sextics with coefficients in $\{-10^{12}, \dots, 10^{12}\}$ uniformly distributed

2	3	1	4	(11)	(11)1	5	(21)	(11)2	6	(11)3	(21)1	(31)	7
29.12%	25.77%	16.44%	11.06%	8.02%	4.30%	2.46%	1.19%	0.98%	0.30%	0.13%	0.12%	0.07%	0.02%

Table 5: Sextics that are determinants of random symmetric matrices with linear entries

n	1	\emptyset	2	(11)	3
10	90.17%	5.14%	4.50%	0.09%	0.09%
11	89.95%	4.75%	5.06%	0.12%	0.12%
12	89.90%	4.28%	5.53%	0.15%	0.15%

Table 6: Sextics that are signed sums of n sixth powers of linear forms

If we naively sample our sextics having uniformly distributed integer coefficients, then the empirical distribution is even more skewed (Table 3). In Table 4 we see the empirical distribution obtained from sampling symmetric sextic polynomials. We do this by taking linear combinations of the monomial symmetric polynomials with coefficients being uniformly distributed integers between -10^{12} and 10^{12} . We see that the distribution now looks rather different from the two distributions considered before. For example, Type 7 appears with probability 0.01% whereas it did not appear among the 1,500,000 samples from the $U(3)$ -invariant distribution. The largest variety of types is observed when we sample sextics of the form $\det(xA + yB + zC)$ where A, B and C are symmetric 6×6 -matrices whose entries are uniformly distributed random integers between -1000 and 1000 (Table 5). This is also the only distribution we considered where the type with only one oval is not the most common type. Several types appear that did not show up among the 1,500,000 samples in Table 2.

Our most skewed distribution was from sampling signed sums (with the signs chosen uniformly at random) of ten sixth powers of linear forms whose coefficients are uniformly distributed integers between -1000 and 1000 . Thus, here we are restricting to sextics of real rank 10, the case considered in [27, §6]. Table 6 reveals that more than 90% of the samples have one oval. After passing to eleven summands, we observe more curves of Type 2 than empty curves. Going to sums of twelve sixth powers of linear forms increases this effect.

Our experiments demonstrate that it is extremely rare to observe many ovals when sextic curves are generated at random. We never encountered a sextic with 8, 9, 10 or 11 ovals. Only few types occurred in our samples. This underscores the importance of having the explicit polynomials in $\mathbb{Z}[x, y, z]_6$ that are listed above, to serve as seeds for local sampling.

4 Constructing Representatives

In this section we discuss the construction of representative sextics, such as those listed in Section 2. We also present a method for sampling from any of the 64 rigid isotopy classes.

Small coefficient size is a natural criterion for desirable representatives. We say that a sextic f as in (7) is *optimal* if its coefficients c_{ijk} are integers, its complex curve $V_{\mathbb{C}}(f)$ is smooth, and the largest absolute value $|c_{ijk}|$ is minimal among all such sextics in the same rigid isotopy class. For instance, the Fermat sextics $x^6 + y^6 \pm z^6$ are optimal. One approach to finding optimal sextics is to sample at random from sextics with $|c_{ijk}| \in \{0, 1, \dots, m\}$ with m very small. One might also do a brute force search that progressively increases the sum of the absolute values $|c_{ijk}|$. Such strategies work for some of the types seen with highest frequency in Table 2. For instance, sampling with $m = 1$ yields these four optimal sextics:

$$\begin{array}{ll}
2 & \text{nd} \quad x^6 - x^5y - x^5z - x^4yz + x^3y^3 + x^3yz^2 - x^2y^4 - x^2y^2z^2 + xy^4z \\
& \quad -xy^3z^2 - xy^2z^3 - xyz^4 + y^6 + y^5z + y^4z^2 + y^3z^3 - yz^5 + z^6 \\
3 & \text{nd} \quad x^6 - x^5y - x^4y^2 + x^4z^2 + x^3y^3 + x^3y^2z + x^3yz^2 + x^2y^3z - x^2y^2z^2 + x^2yz^3 + x^2z^4 \\
& \quad +xy^4z + xy^3z^2 + xy^2z^3 + xyz^4 - xz^5 + y^6 + y^5z + y^4z^2 - y^2z^4 - yz^5 + z^6 \\
(11) & \text{nd} \quad x^5y + x^5z + x^4y^2 + x^4yz - x^3y^3 + x^3yz^2 - x^3z^3 - x^2y^4 + x^2y^3z + x^2y^2z^2 - x^2yz^3 \\
& \quad +x^2z^4 - xy^4z + xy^3z^2 - xyz^4 + xz^5 - y^5z - y^4z^2 + y^3z^3 + y^2z^4 - yz^5 - z^6 \\
4 & \text{nd} \quad -x^6 + x^5y + x^4y^2 - x^3y^3 + x^2y^4 + xy^5 - y^6 + x^5z + x^4yz + xy^4z \\
& \quad +y^5z + x^4z^2 + y^4z^2 - x^3z^3 - y^3z^3 + x^2z^4 + xyz^4 + y^2z^4 + xz^5 + yz^5 - z^6
\end{array}$$

However, this approach is not useful for constructing the vast majority of types, since these are extremely rare when we sample at random, and they will never appear for small m .

For all systematic constructions, it is imperative to work with the *discriminant* Δ . Each connected component of the complement $\mathbb{R}[x, y, z]_6 \setminus \Delta$ corresponds to one of our 64 types. We identify Δ with its defining irreducible polynomial over \mathbb{Z} in the 28 unknowns c_{ijk} .

We evaluate Δ using *Sylvester's formula*, as stated by Gelfand, Kapranov and Zelevinsky [13, Theorem 4.10, Chapter 3]. This expresses Δ as the determinant of a 45×45 -matrix \mathcal{S}_f . Each entry in the first 30 columns of \mathcal{S}_f is either 0 or one of the coefficients c_{ijk} . The entries in the last 15 columns are cubics in the c_{ijk} . So, the degree of $\det(\mathcal{S}_f)$ is 75, as required. The *Sylvester matrix* \mathcal{S}_f is the representation in monomial bases of an \mathbb{R} -linear map

$$\mathcal{S}_f : (\mathbb{R}[x, y, z]_3)^3 \oplus \mathbb{R}[x, y, z]_4 \longrightarrow \mathbb{R}[x, y, z]_8$$

that is defined as follows. On the first summand, it maps a triple of cubics to an octic via

$$\mathcal{S}_f : (a, b, c) \mapsto a \frac{\partial f}{\partial x} + b \frac{\partial f}{\partial y} + c \frac{\partial f}{\partial z}.$$

On the second summand, the map \mathcal{S}_f takes a quartic monomial $x^r y^s z^t$ to the octic $\det(M_{rst})$, where M_{rst} is any 3×3 -matrix of ternary forms that satisfies the homogeneous identity

$$\begin{pmatrix} \partial f / \partial x \\ \partial f / \partial y \\ \partial f / \partial z \end{pmatrix} = M_{rst} \cdot \begin{pmatrix} x^{r+1} \\ y^{s+1} \\ z^{t+1} \end{pmatrix}.$$

The entries of M_{rst} are linear in the c_{ijk} , so $\det(M_{rst})$ is an octic in x, y, z whose coefficients are cubics in the c_{ijk} . These are the entries in the column of \mathcal{S}_f that is indexed by $x^r y^s z^t$.

Proposition 4.1. *The discriminant Δ equals the determinant of the 45×45 -matrix \mathcal{S}_f .*

Proof. We use Sylvester's formula for the resultant of three ternary quintics. This is [13, Theorem III.4.10] for $d = 5$ and $k = 4$. If we take the three quintics to be the three partial derivatives of f , then we get the matrix \mathcal{S}_f above. That resultant equals our discriminant because both are non-zero homogeneous polynomials of the same degree 75 in the c_{ijk} . \square

A pencil of sextics is a line $\{f + tg\}$ in the space \mathbb{P}^{27} of all sextics. Its discriminant $\Delta(f + tg)$ is a univariate polynomial in t of degree 75. We can compute that polynomial as the determinant of the Sylvester matrix \mathcal{S}_{f+tg} . For two sextics f and g in $\mathbb{Z}[x, y, z]_6$ with reasonable coefficients, we obtain the discriminant $\Delta(f + tg)$ in a few seconds. This method works, in principle, also for evaluating Δ on families with more than one parameter. For instance, we get the output (6) from the input (4) in under one second. However, that output factors and is small. In our experience, the symbolic evaluation of the 45×45 determinant in Proposition 4.1 works well for pencils of sextics, but generally fails for nets of sextics.

Sylvester's formula allows us to sample from a fixed rigid isotopy class. Namely, we start with a representative f with $\Delta(f) \neq 0$, like one of the 64 sextics in Section 2. We then pick a random sextic g and we compute the univariate polynomial $\Delta(f + tg)$. This has 75 complex roots. We extract the real roots, and we identify the largest negative root and the smallest positive root. For any t in the open interval between these two roots, the sextic $f + tg$ has the same rigid isotopy type as f . Repeating this many times, we thus sample from the connected component of $\mathbb{R}[x, y, z]_6 \setminus \Delta$ that contains f . This gives us access to all sextics in the largest star domain with center f contained in that component. We call this process the *local exploration method*. It will be used for the applications in Sections 5 and 6.

For exploring the 64 connected components of $\mathbb{P}_{\mathbb{R}}^{27} \setminus \Delta$, it is important to understand their adjacencies. A general point in the discriminant Δ is a sextic curve f that has precisely one ordinary node. If f is in the real locus $\Delta_{\mathbb{R}}$, then that node is a point in the real plane $\mathbb{P}_{\mathbb{R}}^2$. Two of the 64 types are connected by a *discriminantal transition* if there is a curve in the closure of both of the components having only one singular point which is an ordinary node.

There are three different types of discriminantal transitions. If the singular curve has an isolated real point (acnode), defined locally by $x^2 + y^2 = 0$, then the transition corresponds

to removing one of the empty ovals. We call this operation *shrinking of ovals*. Itenberg [18] uses the term *contraction*. The inverse operation is adding an empty oval.

The following lemma and the subsequent theorem are probably well-known to experts in the area. We include the proofs for lack of a suitable reference.

Lemma 4.2. *Shrinking an oval always leads to a curve of non-dividing type.*

Proof. Consider a real plane curve C with only one singularity p that is an acnode. Since being of non-dividing type is an open condition, we can assume that C is of dividing type. Then p is in the closure of both connected components of $C_{\mathbb{C}} \setminus C_{\mathbb{R}}$. In particular, $(C_{\mathbb{C}} \setminus C_{\mathbb{R}}) \cup \{p\}$ is connected. Therefore, after shrinking an oval we get a curve of non-dividing type. \square

The other type of ordinary node consists of two crossing real branches (crunode), defined locally by $x^2 - y^2 = 0$. There are two possibilities: The connected component containing the node is either two ovals intersecting in one point, or two pseudolines intersecting in one point. The case of one oval and one pseudoline cannot occur in even degree. In the following we describe the topology of small perturbations of the nodal curve in each of these two cases. In the former case, the transition consists of two ovals coming together and forming one oval. This happens in one connected component of the complement of all other ovals. We call this transition *fusing of ovals*. Itenberg [18] uses the term *conjunction*. This operation reduces the number of ovals by one. When two pseudolines intersect, every small perturbation of the nodal curve has the same number of ovals but the interior and exterior of one outermost oval are exchanged. We call this operation *turning inside out*. An example of turning inside out is shown in Figure 3. For plane conics, turning inside out is the only possibility. For quartics, all three transitions are possible. We summarize our discussion as follows.

Theorem 4.3. *For curves of even degree, every discriminantal transition between rigid isotopy types is one of the following: shrinking of ovals, fusing of ovals, and turning inside out.*

Proof. Let C be a real plane curve of even degree with exactly one ordinary singularity p . If p is an acnode, then C corresponds to shrinking. Let p be a crunode. There are two subsets $C_1, C_2 \subset C_{\mathbb{R}}$, both homeomorphic to the circle, such that $C_1 \cap C_2 = \{p\}$. Let $\pi : \tilde{C} \rightarrow C$ be the normalization map. The fiber $\pi^{-1}(p)$ consists of exactly two points $p_1, p_2 \in \tilde{C}_{\mathbb{R}}$.

Suppose that p_1 and p_2 belong to the same connected component of $\tilde{C}_{\mathbb{R}}$. If C_1 or C_2 does not disconnect $\mathbb{P}_{\mathbb{R}}^2$, there would be a small deformation of C to a smooth curve having (at least) one pseudoline as one of the connected components of its real part. Since this is not possible, both C_1 and C_2 disconnect $\mathbb{P}_{\mathbb{R}}^2$. This case corresponds to fusing of ovals.

Next suppose that p_1 and p_2 belong to different connected components of $\tilde{C}_{\mathbb{R}}$. For both bifurcations of the node, the number of connected components of the real part of the curve stays the same. If C_1 or C_2 disconnected $\mathbb{P}_{\mathbb{R}}^2$, then there would be another intersection point of C_1 and C_2 besides p . Thus, $\mathbb{P}_{\mathbb{R}}^2 \setminus C_i$ is connected for $i = 1, 2$, and $\mathbb{P}_{\mathbb{R}}^2 \setminus (C_1 \cup C_2)$ has two connected components, both homeomorphic to an open disc. Depending on the bifurcation of the node, one of these connected components is still homeomorphic to an open disc after deformation and the other one is not. This corresponds to turning inside out. \square

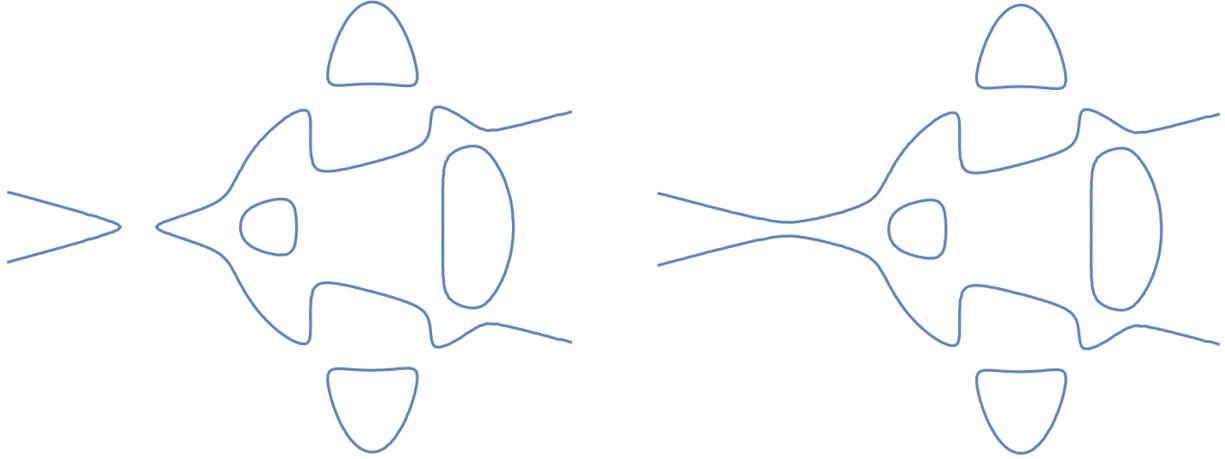


Figure 3: Type (21)2d transitions into Type (21)2nd by turning an oval inside out.

It is instructive to examine the diagram in Figure 1 from the perspective of discriminantal transitions. The edges in the poset correspond to shrinking or fusing. There are three possibilities for what might be geometrically possible: shrinking only, fusing only, or shrinking and fusing. For instance, Type (11) can become Type 1 by either shrinking the inner oval, or by fusing the two nested ovals. Both possibilities are geometrically realized by a singular curve with a single node that lies in the common boundary between the two types.

Theorem 4.4 (Itenberg). *Each of the edges in Figure 1 is realized by shrinking an empty oval, except the one between (hyp) and (11). Not every edge is realized by fusing two ovals.*

Proof. The first statement is [18, Prop. 2.1]. Furthermore, it was shown in [18] that the transition from (11)9 to 10 cannot be realized by fusing. \square

One possible way of explicitly realizing edges by fusing is to use Gudkov's constructions [16] and the following lemma which is a special case of a theorem due to Brusotti [6].

Lemma 4.5. *Let $C_1, C_2 \subset \mathbb{P}^2$ be two smooth real curves of degrees 2 and 4 (resp. 1 and 5) intersecting transversally. By a small perturbation, we can fix any one of the real nodes of the sextic curve $C_1 \cup C_2$ and perturb all the others independently in any prescribed manner.*

Proof. Let $q, p_1, \dots, p_7 \in \mathbb{P}_{\mathbb{R}}^2$ be eight distinct real points lying on the smooth quadric C_1 . We claim that, for every tuple $\epsilon \in \{\pm 1\}^7$, there is a sextic which is singular at q and whose sign at p_i is ϵ_i . Let L be the linear system of all sextic curves that are singular at q . The pull-back of L to $C_1 \cong \mathbb{P}^1$ is the set of all bivariate forms of degree 12 having a double root at q . Since for any distinct 7 points in \mathbb{R} there is a polynomial of degree 10 that vanishes on all but one of these points, the claim follows. The other case (degrees 1 and 5) is analogous. \square

We might also approach these questions by computational means. This requires a software tool for the following task. Consider two general sextics $f, g \in \mathbb{Z}[x, y, z]_6$ and compute the

univariate polynomial $\Delta(f + tg)$ of degree 75. For each of its real roots t^* , we must decide if the transition at t^* is a shrinking of ovals, a fusing of ovals, or turning inside out.

Let us now examine our third discriminantal transition. Turning inside out preserves the number of ovals, so it is an operation that acts on each of the rows in Figure 1 separately.

Proposition 4.6. *If we turn an outermost oval of a smooth sextic inside out, then the topological type of the resulting curve is the one obtained by reflecting Figure 1 vertically. If the curve was dividing, then it is non-dividing after turning inside out. Curves that are non-dividing can become either dividing or non-dividing.*

Proof. Let C be a real plane curve with exactly one ordinary crunode p . In a neighborhood of p , the Riemann surface $C_{\mathbb{C}}$ is homeomorphic to the union of two discs D_1 and D_2 with $D_1 \cap D_2 = \{p\}$. The real part $C_{\mathbb{R}}$ divides D_1 and D_2 into two connected components D_1^+ , D_1^- and D_2^+ , D_2^- respectively. One of the two possible smoothenings of the node p connects D_1^+ with D_2^+ and the other one connects D_1^+ with D_2^- . Thus, if C is dividing then exactly one of the two deformations results in a dividing curve. Otherwise, both are non-dividing. \square

Not every vertical reflection in Figure 1 can be realized geometrically by a discriminantal transition. For instance, the types (91)1 and (11)9 are related by a vertical reflection. But both types are dividing, so Proposition 4.6 implies that they are not connected by turning inside out. Put differently, these two components of $\mathbb{P}_{\mathbb{R}}^{27} \setminus \Delta$ do not share a wall of codimension one. In fact, turning inside out can only happen for curves with at most 9 ovals. Indeed, consider a plane sextic curve with exactly one crunode and r connected components, one of which is the intersection of two pseudolines. The normalization of such a curve has genus 9 and $r + 1$ connected components. By Harnack's inequality this implies that $r \leq 9$.

We now come to the punchline of Section 4, namely, how the polynomials in Section 2 were created. An established and powerful technique for constructing real varieties with prescribed topology is Viro's *patchworking method* [39]. All 56 topological types of smooth sextics can be realized by a version of patchworking known as *combinatorial patchworking*, which can also be interpreted in the language of tropical geometry. In that guise, one records the signs of the 28 coefficients c_{ijk} and represents their magnitudes by a regular triangulation of the Newton polygon. Transitioning from that representation to actual polynomials in $\mathbb{Z}[x, y, z]_6$ yields integer coefficients c_{ijk} whose absolute values tend to be very large. We experimented with some of these sextics, but in the end we abandoned them for all but three types, because symbolic computation became prohibitively slow.

Instead, for deriving Proposition 2.1, we used that many types, especially the sextics with 3 to 7 ovals, can be found by perturbing the union of three quadrics intersecting transversally. This process is shown in Figure 4. Some of the types with 8 and 9 components could also be constructed in a similar fashion. This is reflected in our representatives in Section 2.

For most other types, we carried out the classical constructions of Harnack and Hilbert, as explained by Gudkov [16]. We start with two quadrics intersecting in four real points, pick eight points on the curves, and perturb the reducible quartic with the product of four lines through these points. The smooth quartic is intersected with one of the original quadrics and perturbed again to get a smooth sextic. The different ways in which the original curves

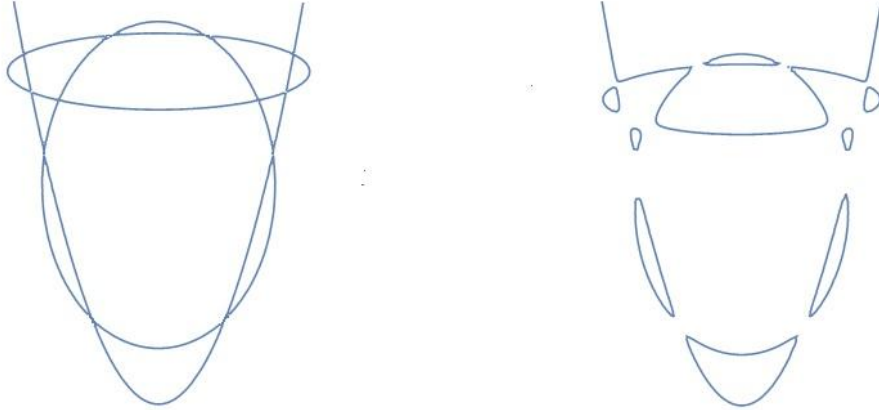


Figure 4: A sextic of Type (11)7 is constructed by perturbing the union of three quadrics.

and the points on them are selected give the different types. This method worked for almost all types. For the construction of type (51)5, we tried Gudkov's method but found it too complicated to carry out explicitly. We employed Viro's method in [37, §3.2] and built a curve of type (51)5 using patchworking on three touching ellipses.

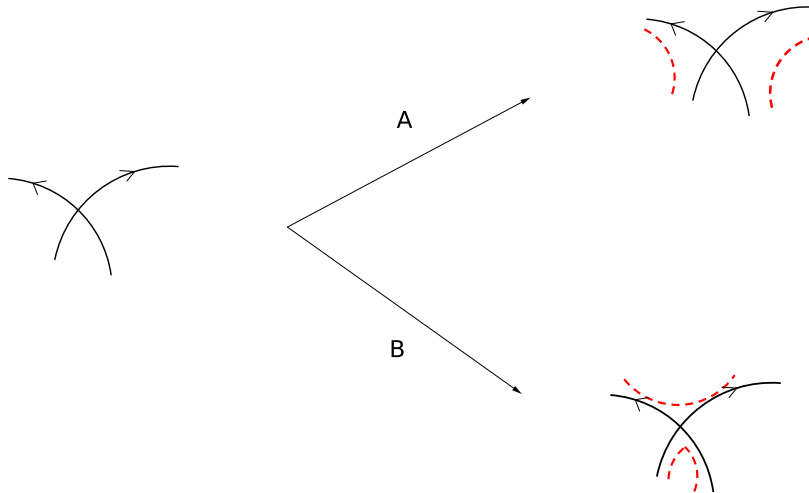


Figure 5: Using local perturbations to create sextics that are dividing or non-dividing

These constructions enabled us to find representatives for the 56 topological types. What remained was the issue of distinguishing between dividing and non-dividing curves. In particular, we needed to find two representatives for the pairs of rigid isotopy types in the eight Nikulin cases (1). To construct those, we considered dividing curves of degree d_1 and d_2 , with prescribed orientations, that intersect in $d_1 \cdot d_2$ real points. The singular points of the reducible curve can be made smooth in two ways, shown in red in Figure 5. According to Fiedler [14, §2], if *all* intersections are perturbed either using only A or using only B then it is dividing. However, if the smoothening is done via A at some crossings and via B at

other crossings, then the resulting smooth curve does not divide its Riemann surface. In particular, for the construction of types (41)4d and (41)4nd we followed [12, page 273].

At this point, we had 64 representative sextics, and each of them was certified by our code `SexticClassifier`. However, the coefficient size for most of them was still unsatisfactory. To improve the representatives, and to arrive at the list that is displayed in Section 2, Sylvester’s formula for the discriminant (Proposition 4.1) proved again to be very helpful.

There are basically two heuristical methods that we used. One is to shrink the absolute value of each coefficient of a given representative separately as far as possible without crossing the discriminant locus. The other way is to choose a prime number p and vary the polynomial without crossing the discriminant locus so that every coefficient of the resulting polynomial is divisible by p . In our experience, a combination of the two methods yields the best results.

5 Avoidance Locus, Dual Curve, and Bitangents

Many software packages for plane curves, such as those discussed at the beginning of Section 3, work with affine coordinates. They often assume that the given curve is compact, so its closure in $\mathbb{P}_{\mathbb{R}}^2$ is disjoint from a distinguished line, namely, the line at infinity. We saw in Example 3.1 that no such line exists for some sextics. This motivates the concept of the avoidance locus, to be introduced and studied in this section. This will lead us naturally to computing dual curves and bitangent lines, and to investigating the reality of these objects.

Let C be a smooth real curve of even degree d in \mathbb{P}^2 . Its *avoidance locus* is the set \mathcal{A}_C of all lines in $\mathbb{P}_{\mathbb{R}}^2$ that do not intersect the real curve $C_{\mathbb{R}}$. Thus, \mathcal{A}_C is a semi-algebraic subset of the dual projective plane $(\mathbb{P}^2)_{\mathbb{R}}^{\vee}$. We write C^{\vee} for the curve of degree $d(d-1)$ in $(\mathbb{P}^2)^{\vee}$ that is dual to C . The points on C^{\vee} correspond to lines in \mathbb{P}^2 that are tangent to C . The real dual curve $C_{\mathbb{R}}^{\vee}$ divides the real projective plane $(\mathbb{P}^2)_{\mathbb{R}}^{\vee}$ into connected components.

Proposition 5.1. *Up to closure, the avoidance locus \mathcal{A}_C is a union of connected components of $(\mathbb{P}^2)_{\mathbb{R}}^{\vee} \setminus C_{\mathbb{R}}^{\vee}$. Each component appearing in \mathcal{A}_C is convex, when regarded as a cone in \mathbb{R}^3 .*

Proof. Points in $(\mathbb{P}^2)_{\mathbb{R}}^{\vee} \setminus C_{\mathbb{R}}^{\vee}$ correspond to real lines that intersect C transversally. Whether that intersection contains real points or not does not change unless the curve $C_{\mathbb{R}}^{\vee}$ is crossed. Hence $\mathcal{A}_C \setminus C_{\mathbb{R}}^{\vee}$ is a union of connected components of $(\mathbb{P}^2)_{\mathbb{R}}^{\vee} \setminus C_{\mathbb{R}}^{\vee}$. Each such component is convex: it is the convex dual of the convex hull of $C_{\mathbb{R}}$ in the affine space $\mathbb{P}_{\mathbb{R}}^2 \setminus L$, where $L \in \mathcal{A}_C$. The prefix “up to closure” is needed because \mathcal{A}_C also contains some points in $C_{\mathbb{R}}^{\vee}$, corresponding to real lines that do not meet $C_{\mathbb{R}}$ but are tangent to C at complex points. \square

Example 5.2. Let $d = 4$ and consider the *Edge quartic* C , taken from [30, equation (1.5)]:

$$25(x^4 + y^4 + z^4) - 34(x^2y^2 + x^2z^2 + y^2z^2) = 0.$$

This curve $C \subset \mathbb{P}^2$ served as a running example in [30]. It is shown on the left in Figure 6. We choose coordinates $(u : v : w)$ for points in the dual projective plane $(\mathbb{P}^2)^{\vee}$. Such a point

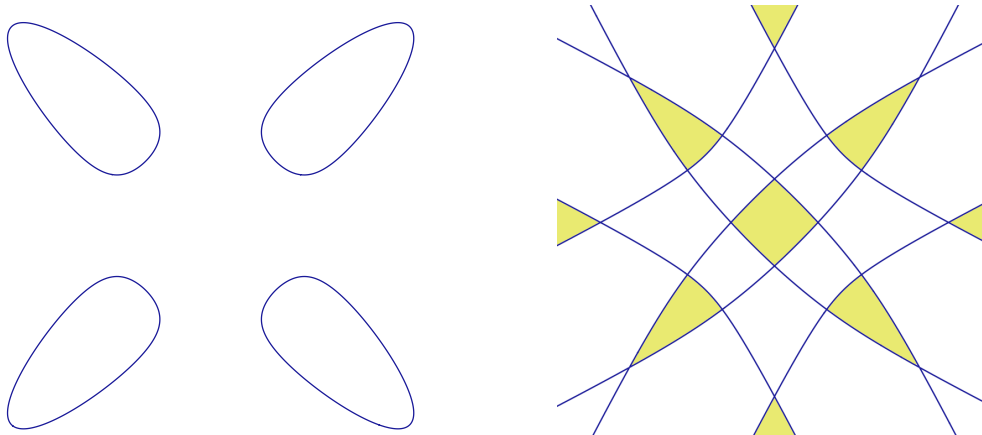


Figure 6: The Edge quartic C and its dual C^\vee ; the avoidance locus \mathcal{A}_C is colored.

represents the line $L = \{ux + vy + wz = 0\}$ in the primal \mathbb{P}^2 . The dual curve C^\vee is given by

$$\begin{aligned}
& 10000u^{12} - 98600u^{10}v^2 - 98600u^{10}w^2 + 326225u^8v^4 + 85646u^8v^2w^2 + 326225u^8w^4 - 442850u^6v^6 \\
& - 120462u^6v^4w^2 - 120462u^6v^2w^4 - 442850u^6w^6 + 326225u^4v^8 - 120462u^4v^6w^2 + 398634u^4v^4w^4 \\
& - 120462u^4v^2w^6 + 326225u^4w^8 - 98600u^2v^{10} + 85646u^2v^8w^2 - 120462u^2v^6w^4 - 120462u^2v^4w^6 \\
& + 85646u^2v^2w^8 - 98600u^2w^{10} + 10000v^{12} - 98600v^{10}w^2 + 326225v^8w^4 - 442850v^6w^6 + 326225v^4w^8 \\
& - 98600v^2w^{10} + 10000w^{12} = 0.
\end{aligned}$$

The dual curve $C_{\mathbb{R}}^\vee$ divides $(\mathbb{P}^2)_{\mathbb{R}}^\vee$ into 21 open regions. Seven of the regions comprise the avoidance locus \mathcal{A}_C . They are colored in Figure 6, and they represent the seven ways of bipartitioning the four ovals of $C_{\mathbb{R}}$ by a straight line. The convex body dual to the convex hull of $C_{\mathbb{R}}$, in our affine drawing on the left, is the innermost yellow region on the right. \diamond

The number seven of yellow regions seen in Figure 6 attains the following upper bound.

Proposition 5.3. *Let C be a smooth real curve of even degree d in \mathbb{P}^2 . The number of open convex sets in the dual plane that make up the avoidance locus \mathcal{A}_C is bounded above by*

$$\frac{9}{128}d^4 - \frac{9}{32}d^3 + \frac{15}{32}d^2 - \frac{3}{8}d + 1. \quad (8)$$

Proof. By Harnack's inequality, $C_{\mathbb{R}}$ can have at most $\binom{d-1}{2} + 1$ ovals in $\mathbb{P}_{\mathbb{R}}^2$. However, for our count we only care about the outermost ovals, i.e. those not contained inside any other oval. By a result of Arnold in [2], which is a more precise version of a classical inequality due to Petrovsky [29], the number of outermost ovals of the curve $C_{\mathbb{R}}$ is at most

$$m = \frac{3}{8}d^2 - \frac{3}{4}d + 1.$$

Pick a generic point in each oval. Then the configuration of points has $\binom{m}{2} + 1$ bipartitions that can be realized by a straight line. Indeed, dually, this is the number of regions in the complement of a general arrangement of m lines in the plane $\mathbb{P}_{\mathbb{R}}^2$. The quartic polynomial

in (8) is simply $\binom{m}{2} + 1$ with Petrovsky's expression for m . It remains to be seen that this number is the desired upper bound. Indeed, every connected component of \mathcal{A}_C is uniquely labeled by a bipartition of the set of non-nested ovals. The number of such bipartitions that are realized by a straight line is bounded above by the said bipartitions of the points. \square

The upper bound in (8) evaluates to 46 for $d = 6$. Here is a sextic that attains the bound.

Example 5.4. Let t and ϵ be parameters, and consider the following net of sextics:

$$\begin{aligned} F_{t,\epsilon} = & 60x^6 - 750x^5z - 111x^4y^2 + 1820x^4z^2 + 700x^3y^2z - 2250x^3z^3 + 20x^2y^4 \\ & - 1297x^2y^2z^2 + 960x^2z^4 - 56xy^4z + 1440xy^2z^3 - y^6 - 576y^2z^4 \\ & + t(x^3 + xz^2 - y^2z)^2 + \epsilon(x^2z^4 + y^2z^4 + z^6) \end{aligned}$$

For $t_0 = -\frac{1645}{2} - 150\sqrt{34}$ and $\epsilon = 0$, the sextic $F_{t_0,0}$ has 10 isolated real singular points:

$$((3 - \sqrt{34})/5 : 0 : 1), (0 : 0 : 1), (1 : \pm\sqrt{2} : 1), (2 : \pm\sqrt{10} : 1), (3 : \pm\sqrt{30} : 1), (4 : \pm 2\sqrt{17} : 1).$$

No three of these 10 points lie on a line. For any sufficiently small $\epsilon > 0$ and t sufficiently close to t_0 , the sextic $F_{t,\epsilon}$ is smooth with 10 small ovals arranged around the singular points of $F_{t_0,0}$. When these ovals are small enough, the avoidance locus will have the maximum number 46 of connected components, by the argument given in the proof of Proposition 5.3. This example was found using the construction developed by Kunert and Scheiderer in [23].

We now describe an algorithm for computing the avoidance locus \mathcal{A}_C of a smooth curve C . The first step is to find all bitangents of C . A *bitangent* of C is a line L in \mathbb{P}^2 that is tangent to C at two points. Note that bitangents of C correspond to nodal singularities of the dual curve C^\vee . By the Plücker formulas, the expected number of bitangents is $(d-3)(d-2)d(d+3)/2$, which is 324 for $d = 6$. A bitangent L is called *relevant* if the real part of the divisor $L \cap C$ is an even divisor on the curve C . For generic curves C , this means that L has no real intersection points with C except possibly the two points of tangency. If these two points are real, then L is an extreme point of a convex connected component of \mathcal{A}_C .

Remark 5.5. Let C be a smooth curve in $\mathbb{P}_{\mathbb{R}}^2$ of degree $d \geq 4$. If C contains at least two outermost ovals or has a non-convex outermost oval, then every connected component of the avoidance locus \mathcal{A}_C has a relevant bitangent in its closure. If C does not satisfy this hypothesis then \mathcal{A}_C is connected; we do not know whether it always contains a real bitangent. In the case of quartics, this follows from the Zeuthen classification [30, Table 1]. In that case, however, the number of bitangents only depends on the topological type. In higher degrees, when this is not the case, not much seems known. (See Conjecture 5.8 below.)

We now assume that C satisfies the hypothesis in Remark 5.5. Our algorithm for computing \mathcal{A}_C is as follows. First we compute linear forms representing all real bitangents of C , and we discard those that are not relevant. Next, we compute a graph \mathcal{G}_C whose nodes are the relevant bitangents, as follows: two linear forms L_1 and L_2 form an edge if and only if

- (a) $L_1 + L_2$ lies in the avoidance locus \mathcal{A}_C , and

(b) the open line segment $\{tL_1 + (1-t)L_2 : 0 < t < 1\}$ is disjoint from the dual curve $C_{\mathbb{R}}^{\vee}$.

Here the sign of the linear forms L_1 and L_2 for the bitangents has to be chosen carefully.

Remark 5.6. The graph \mathcal{G}_C is a disjoint union of cliques, one for each connected component of \mathcal{A}_C . This follows from Remark 5.5 and convexity of the connected components.

In summary, given a smooth curve $C = V_{\mathbb{C}}(f)$ of even degree d , our algorithm computes the *avoidance graph* \mathcal{G}_C . We represent the avoidance locus \mathcal{A}_C by the connected components (cliques) of \mathcal{G}_C . Midpoints of the segments in (b) furnish sample points in the components.

We made a proof-of-concept implementation of this algorithm for the case of sextics. Its two main ingredients are computing the dual curve and computing the bitangents. For the former task we solve a linear system of equations in the $\binom{30+2}{2} = 496$ coefficients of C^{\vee} . The equations are derived by projecting C from random points $p \in \mathbb{P}^2$. The ramification locus of this projection reveals (up to scaling) the binary form of degree 30 that defines $C^{\vee} \cap p^{\perp}$.

To compute the bitangents, we employ the variety of binary sextics with two double roots. The prime ideal of this variety is defined by 13 forms of degree 7; see the row labeled 2211 in [24, Table 1]. Substituting the binary form $f(x, y, -\frac{1}{w}(ux + vy))$ into that ideal, and clearing denominators, yields the ideal in $\mathbb{Q}[u, v, w]$ that defines the 324 bitangents $(u:v:w) \in (\mathbb{P}^2)^{\vee}$.

Example 5.7. Let C be the representative for Type 8nd displayed in Section 2. This sextic curve has 324 distinct complex bitangents of which 124 are real. Of the real bitangents,

- 8 are tangent at non-real points and meet the curve in two more non-real points;
- 60 are tangent at real points and meet the curve in two more non-real points;
- 4 are tangent at non-real points and meet the curve in two more real points;
- 52 are tangent at real points and meet the curve in two more real points.

Only the first two types are relevant, so C has 68 relevant bitangents. The avoidance graph \mathcal{G}_C is found to consist of 14 cliques: four K_6 's, five K_5 's, four K_4 's and one K_3 . Hence \mathcal{A}_C consists of 14 convex components. The curve C together with its 68 relevant bitangents is shown in Figure 7. There are 14 ways to bipartition the 8 ovals by a line that avoids $C_{\mathbb{R}}$.

While the nodes on C^{\vee} are bitangents of C , the cusps on C^{\vee} are the *flex lines* of C . The number of *inflection points* is $3d(d-2)$ for a general curve of degree d . A classical result due to Felix Klein states that at most one third of the complex inflection points of a real plane curve can be real. Brugallé and López de Medrano [5] proved, using tropical methods, that Klein's upper bound $d(d-2)$ is attained for all $d \geq 3$. Hence, for smooth sextics, the number of real inflection points can be any even integer between 0 and 24. The distribution of the numbers of real bitangents and real inflection points over the 64 rigid isotopy types is presented in Section 6. Based on our experiments, we propose the following conjecture:

Conjecture 5.8. *The number of real bitangents of a smooth sextic in $\mathbb{P}_{\mathbb{R}}^2$ ranges from 12 to 306. The lower bound is attained by curves in the following four types: empty, 1, 2, (11) and (hyp). The upper bound is attained by certain 11-oval curves of Gudkov-type (51)5.*

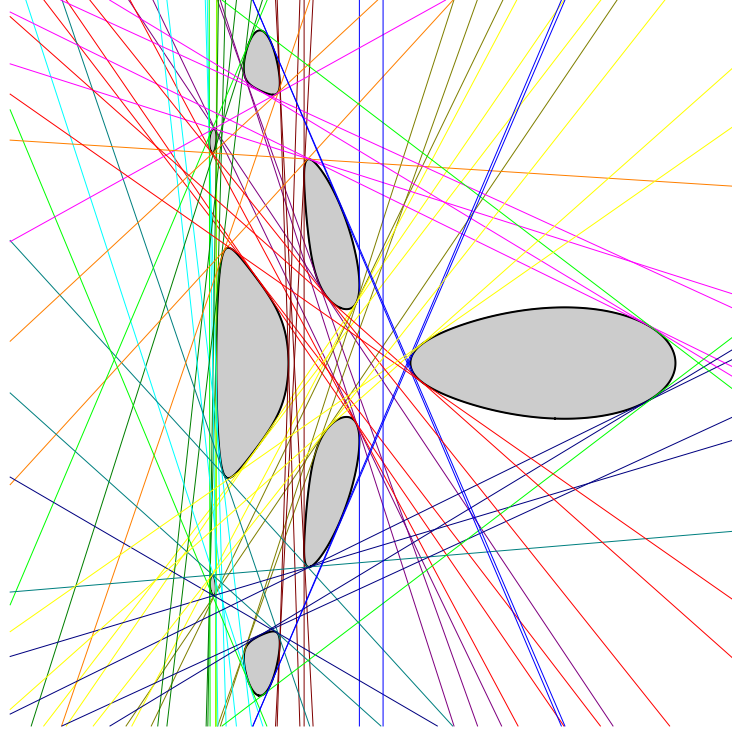


Figure 7: A sextic curve C with 8 non-nested ovals; its 68 relevant bitangents represent \mathcal{A}_C .

The numbers of real inflection points and bitangents of a sextic C often change when passing through the discriminant hypersurface. However, they may also change within the same rigid isotopy type. If C is smooth then the total number of complex inflection points resp. bitangents drops below the bounds 72 resp. 324 in the following three exceptional cases:

- (411) C has an *undulation point*, in which the tangent meets C with multiplicity at least 4.
- (222) C has a *tritangent line*, i.e. a line that is tangent to C in three distinct points.
- (321) C has a *flex-bitangent*, i.e. a line that meets C with multiplicity 3 in one point and is tangent at another point.

In each case, the stated property defines a hypersurface in $V = \mathbb{R}[x, y, z]_6$. The number of real inflection points or bitangents changes only when passing through the discriminant or one of these hypersurfaces. When generic sextics approach these hypersurfaces, three lines come together: a bitangent and two flex lines for an undulation point (411), three bitangents for a tritangent line (222), and two bitangents and a flex line for a flex-bitangent (321).

Theorem 5.9. *Let \mathcal{T} be the Zariski closure in $\mathbb{P}V = \mathbb{P}^{27}$ of the set of smooth sextics with a tritangent line and let \mathcal{F} be the locus of smooth sextics with a flex-bitangent. Then:*

1. *The loci \mathcal{T} and \mathcal{F} are irreducible hypersurfaces of degree 1224 and 306 respectively.*
2. *Their union $\mathcal{B} = \mathcal{T} \cup \mathcal{F}$ is the bitangent discriminant, i.e. the Zariski closure of the set of smooth sextics in $\mathbb{P}V$ having fewer than 324 bitangent lines.*

Proof. The variety of binary sextics with three double roots is irreducible of codimension 3 in $\mathbb{R}[x, y]_6$. (It is defined by 45 quartics [24, Table 1].) Let \mathcal{X} be the incidence variety of all pairs (L, f) in $(\mathbb{P}^2)^\vee \times \mathbb{P}V$ where L is a tritangent of $V_{\mathbb{C}}(f)$. The locus \mathcal{T} is the projection of \mathcal{X} onto $\mathbb{P}V$. The intersection of \mathcal{X} with any subspace of the form $\{L\} \times \mathbb{P}V$ for $L \in (\mathbb{P}^2)^\vee$ has codimension 3 in $\mathbb{P}V$. Taking the union over all L , we conclude that \mathcal{T} has codimension 1. Since the projection of \mathcal{X} onto the first factor is surjective with irreducible fibers of constant dimension, \mathcal{X} is irreducible, hence so is \mathcal{T} . The same argument applies to \mathcal{F} . The degrees of the hypersurfaces \mathcal{F} and \mathcal{T} were computed for us by Israel Vainsencher with the Maple package `schubert`. The relevant theory is described by Colley and Kennedy in [9].

To prove (2), we first note that a tritangent splits into three bitangents, and a flex-bitangent into two bitangents and a flex line, for any smooth deformation of a sextic in \mathcal{T} or \mathcal{F} , respectively. This shows that \mathcal{T} and \mathcal{F} are both contained in the bitangent discriminant. For the reverse, we argue in the dual picture, with degenerations of singularities on C^\vee . \square

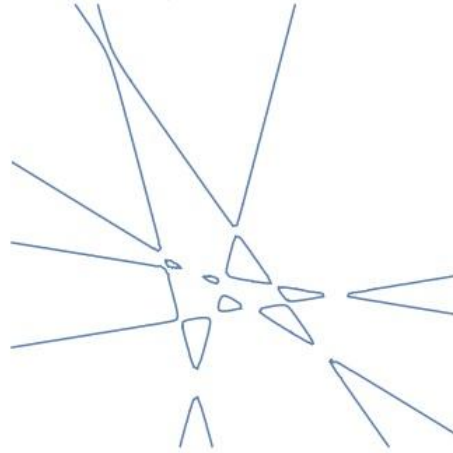


Figure 8: A smooth sextic with 10 non-nested ovals whose avoidance locus is empty

We conclude this section with the following result on the avoidance loci of plane sextics.

Corollary 5.10. *For any integer m between 0 and 46, there exists a smooth sextic C in $\mathbb{P}_{\mathbb{R}}^2$ whose avoidance locus \mathcal{A}_C comprises exactly m convex connected components.*

Proof. Let f_1 be a sextic of Type 10nd whose avoidance locus has 46 components, as in Example 5.4. Let f_0 be a sextic of Type 10nd with empty avoidance locus, for instance

$$f_0 = (20x^2 - (y+10z)^2 + z^2)(21y^2 - (x-10z)^2 + z^2)(20(x-5z+y)^2 - (y+10z)^2 + z^2) + z^6.$$

The real picture of such a curve is shown in Figure 8. Let U be the connected component of $\mathbb{P}_{\mathbb{R}}^{27} \setminus \Delta$ that contains both f_0 and f_1 . Consider the bitangent discriminant \mathcal{B} of Theorem 5.9. There is an open dense subset \mathcal{B}_0 of \mathcal{B} , whose points represent curves with a single tritangent line or a single flex-bitangent. The exceptional locus $Z = \mathcal{B} \setminus \mathcal{B}_0$ has codimension at least 2 in $\mathbb{P}_{\mathbb{R}}^{27}$, hence $V = U \setminus Z$ is path-connected. Fix a path $\gamma: [0, 1] \rightarrow V$ with $\gamma(0) = f_0$, $\gamma(1) = f_1$.

Let $\{\gamma(t_1), \dots, \gamma(t_k)\}$ be its intersection points with \mathcal{B} . Since $\gamma(t_i)$ lies in \mathcal{B}_0 , the number of connected components of the avoidance locus of $V_{\mathbb{R}}(\gamma(t))$ cannot change by more than 1 in a neighborhood of t_i . Indeed, at a point where that number drops by one, exactly three relevant bitangents come together, giving a sextic with a single tritangent in \mathcal{B}_0 . Hence any number of convex avoidance components between 0 and 46 is realized along the path γ . \square

6 Experiments and K3 Surfaces

We begin this section with a report on further experiments on reality questions for plane sextics. Our findings are summarized in Table 7. Thereafter, we discuss implications for real K3 surfaces, and we show how to construct quartic surfaces in $\mathbb{P}_{\mathbb{R}}^3$ with prescribed topology.

Table 7 summarizes experimental data on the numbers of real features associated with real sextics in $\mathbb{P}_{\mathbb{R}}^2$. Certified samples were drawn in the vicinity of each of our current 64 representatives, using the local exploration method that is described after Proposition 4.1.

Each row of Table 7 has five entries: the name of the rigid isotopy type, numbers of real inflection points, numbers of real eigenvectors, numbers of real bitangents, and one real rank. The numbers are ranges of integers that were observed in our experiments. For instance, for Type (11)1, we found numbers ranging between 20 and 66 of real bitangents among 324 complex ones. In some cases, all samples gave the same number of real solutions. For instance, all our Type (71) sextics had 108 real bitangents. Each entry in Table 7 can be regarded as a **conjecture**. For example, we conjecture that every smooth sextic of Type (71) has exactly 108 real bitangents. For real inflection points and real eigenvectors we performed exact computations. That means that we are sure that all numbers listed in the table actually occur. However, we do not know whether there are more possible numbers. For bitangents the calculations are more involved and we applied numerical methods. This means that, for some instances, the number of real solutions might be undercounted. This can happen when two or more real bitangents lie very close to each other. The computations for estimating the real rank are even more delicate and were also accomplished numerically.

Bitangents and their applications were discussed in detail in the previous section. We now give the definitions needed to understand the other three columns in Table 7.

The second column concerns *inflection points* of a smooth sextic $V_{\mathbb{C}}(f) \subset \mathbb{P}^2$. There are $72 = 6 \cdot 12$ complex inflection points. They are computed as the solutions of the equations

$$f(x, y, z) = \det \begin{pmatrix} \frac{\partial^2 f}{\partial x^2} & \frac{\partial^2 f}{\partial x \partial y} & \frac{\partial^2 f}{\partial x \partial z} \\ \frac{\partial^2 f}{\partial x \partial y} & \frac{\partial^2 f}{\partial y^2} & \frac{\partial^2 f}{\partial y \partial z} \\ \frac{\partial^2 f}{\partial x \partial z} & \frac{\partial^2 f}{\partial y \partial z} & \frac{\partial^2 f}{\partial z^2} \end{pmatrix} = 0.$$

A curve of degree d has $3d(d-2)$ complex inflection points. A classical result due to Felix Klein states that the number of real inflection points is at most $d(d-2)$. Brugallé and López de Medrano [5] showed that this upper bound is tight for all degrees d . Hence, for a general sextic in $\mathbb{P}_{\mathbb{R}}^2$, the number of real inflection points is an even integer between 0 and 24. The column labeled “Flex” shows the empirical distribution on the 64 rigid isotopy types.

Type	Flex	Eigenvec	Bitang	Rank	Type	Flex	Eigenvec	Bitang	Rank
0	0	3–31	12	3	(11)5nd	6–16	29–31*	116–122	16
1	0–12	3–31*	12–56	3	(11)5d	8–16	25–31*	120–128	16
(11)	0–14	11–31*	12–66	10	7	4–14	25–31*	96–124	14
2	0–8	5–31*	12–52	13	(71)	20–24	29	108	16
(21)	0–10	7–31*	16–86	14	(61)1	20–22	25	104–214	15
(11)1	2–6	7–31*	20–66	15	(51)2	22	25–31	226–228	15
3	0–8	7–31*	24–94	13	(41)3	20	23–25	154–214	14
(hyp)	0–14	11–31*	12–52	13	(31)4	22	21	162–214	14
(31)	2–10	19–31*	24–90	13	(21)5	16–20	29–31	168	13
(21)1	0–6	11–31*	28–72	14	(11)6	12–14	27–31*	172–176	14
(11)2	0–4	11–31*	32–82	13	8	0–12	23–31*	124–142	13
4	0–2	11–31*	36–54	11	(81)nd	18–22	23	122–196	14
(41)nd	14–16	21–31*	48–90	16	(81)d	18–24	29	124–132	12
(41)d	12–14	27–31*	98–104	14	(71)1	14–18	21–31	104–240	13
(31)1	2–8	15–31*	40–86	14	(61)2	18–20	23–31	228–276	13
(21)2nd	10–16	17–31*	54–82	20	(51)3	22	25	192–254	13
(21)2d	8–16	19–31*	60–70	17	(41)4nd	14–16	25	188–220	9
(11)3	8–12	19–31*	48–94	14	(41)4d	18	25	194–230	11
5	2–10	19–31*	52–112	15	(31)5	20	25–31	198–260	13
(51)	12–16	21–31*	54–64	14	(21)6	20	23–31	242–258	15
(41)1	22	27–31*	90–104	14	(11)7	14–16	29–31	216	14
(31)2	14–18	27–31*	126–130	14	9nd	8–16	25–31*	162–172	15
(21)3	16	27–31*	112–116	14	9d	4–16	29–31*	156	15
(11)4	6–10	25–31*	76–106	15	(91)	18–22	23	124–236	13
6	10–12	23–31*	78–108	14	(81)1	16–20	23–31	162–240	14
(61)	16	27–31*	78–88	14	(51)4	20	27	232–234	10
(51)1nd	16	23–25	110–124	15	(41)5	18–20	27–31	232	10
(51)1d	20–24	29	136	16	(11)8	14–18	25–31	142–210	13
(41)2	16–20	29–31	126–128	14	10	0–24	21–31*	192	12
(31)3nd	12	25–31*	124–148	15	(91)1	18–22	25–31	200–284	14
(31)3d	20–22	29	132	16	(51)5	20–22	25–31	276–306	10
(21)4	14–20	27–31*	138–142	15	(11)9	16–20	25–31	174–250	14

Table 7: Computational results for the number of real solutions for inflection points, eigenvectors, bitangents and real rank among the 64 rigid isotopy classes of smooth sextics in $\mathbb{P}_{\mathbb{R}}^2$.

The third and fifth column pertain to the study of tensors in multilinear algebra. Here we identify the space $\mathbb{R}[x, y, z]_6$ of ternary sextics with the space of symmetric tensors of format $3 \times 3 \times 3 \times 3 \times 3 \times 3$. Such a symmetric tensor f has 28 distinct entries, and these are the coefficients c_{ijk} of the sextic. A vector $v \in \mathbb{C}^3$ is an *eigenvector* of f if v is parallel to the gradient of f at v . Thus the eigenvectors correspond to the solutions in $\mathbb{P}_{\mathbb{C}}^2$ of the constraint

$$\text{rank} \begin{pmatrix} x & y & z \\ \frac{\partial f}{\partial x} & \frac{\partial f}{\partial y} & \frac{\partial f}{\partial z} \end{pmatrix} = 1. \quad (9)$$

A general ternary form f of degree d has $d^2 - d + 1$ eigenvectors [1, Theorem 2.1]. The eigenvectors are the critical points of the optimization problem of maximizing f on the unit sphere $\mathbb{S}^2 = \{(x, y, z) \in \mathbb{R}^3 : x^2 + y^2 + z^2 = 1\}$. Since f attains a minimum and a maximum on \mathbb{S}^2 , the number of real eigenvectors is at least 2. We note that the upper bound $d^2 - d + 1$ is attained over \mathbb{R} . If f is a product of d general linear forms, then all its complex eigenvectors are real. This was shown in [1, Theorem 6.1]. For $d = 6$, we conclude that the number of real eigenvectors of a general ternary sextic is an odd integer between 3 and 31. The column labeled ‘‘Eigenvec’’ shows the empirical distribution on the rigid isotopy types. For many rigid isotopy types we found instances that attain the maximal number 31 of real eigenvectors. Among them are the 35 types that have unions of six real lines in general position in their closure. These types are marked with an asterisk next to the number 31. We found these by perturbing each of the four combinatorial types of arrangements of six lines in general position in $\mathbb{P}_{\mathbb{R}}^2$. This search process resulted in 35 of the rigid isotopy types. This is the result stated in Proposition 1.2. The computation we described is the proof.

A theoretical study of real eigenvectors was undertaken by Maccioni in [26]. He proved that the number of real eigenvectors of a ternary form is bounded below by $2\omega + 1$, where ω is the number of ovals. Our findings in the third column of Table 7 confirm this theorem. Moreover, there are seven types where our computations prove the converse, namely that all values between this lower bound and the upper bound 31 are realized in these types.

Every tensor is a sum of rank one tensors. The smallest number of summands needed in such a representation is the *rank* of that tensor. This notion depends on the underlying field. Symmetric tensors of rank 1 are powers of linear forms (times a constant). Hence, the rank r of a ternary form f of degree d is the minimum number of summands in a representation

$$f(x, y, z) = \sum_{i=1}^r \lambda_i (a_i x + b_i y + c_i z)^d. \quad (10)$$

The exact determination of the real rank of a sextic f is very difficult. The task is to decide the solvability over \mathbb{R} of the equations in the unknowns λ_i, a_i, b_i, c_i obtained by equating coefficients in (10). This computation is a challenge for both symbolic and numerical methods. There is no known method that is guaranteed to succeed in practice. If f is a generic sextic in $\mathbb{R}[x, y, z]_6$ then the complex rank of f is 10, and the real rank of f is an integer between 10 and 19. This was shown in [27, Proposition 6.3]. This upper bound is probably not tight.

We experimented with the software `tensorlab` [36]. This is a standard package for tensors, used in the engineering community. This program furnishes a local optimization

method for the following problem: given f and r , find a sextic f^* of rank r that is closest to f , with respect to the Euclidean distance on the tensor space $(\mathbb{R}^3)^{\otimes 6}$. If the output f^* is very close to the input f , we can be confident that f has real rank $\leq r$. If f^* is far from f , even after many tries with different starting parameters, then we believe that f has real rank $\geq r + 1$. However, `tensorlab` does not furnish any guarantees. One needs to rerun the same instance many times to achieve a lower bound on the real rank with high confidence.

The last column of Table 7 suggests the real rank for each of the 64 sextics listed in Section 2. In each case, we report our best guess on the lower bound, based on numerical experiments with that instance. Obtaining these numbers with high confidence proved to be difficult. We had considerable help from Anna Seigal and Emanuele Ventura in carrying this out. Most puzzling is the real rank 20 we found for our representative of type (21)2nd, as this seems to contradict [27, Proposition 6.3]. This is either an error arising in our numerical method, or the sextic lies on some exceptional locus. Clearly, some further study is needed.

We did not yet attempt the same calculation for a larger sample of sextics in each rigid isotopy class. This would be a very interesting future project at the interface of numerics and real algebraic geometry. The guiding problem is to find the maximal generic real rank among sextics. To underscore the challenge, here is another open question: the real rank of the monomial $x^2y^2z^2$ is presently unknown. It is either 11, 12 or 13, by [27, Example 6.7].

We now shift gears and turn to the construction of real K3 surfaces. Two basic models of algebraic K3 surfaces are quartic surfaces in \mathbb{P}^3 and double-covers of \mathbb{P}^2 branched at a sextic curve. Thus, each of our ternary sextics in Section 2 represents a K3 surface over \mathbb{Q} . Suppose we can write $f = v_3^2 - v_2v_4$ where v_i is a form of degree i in x, y, z . Then $F = v_2w^2 + 2v_3w + v_4$ is a quartic in four variables that realizes the K3 surface with one singular point at $(0 : 0 : 0 : 1)$. Blowing up that singular point gives the K3 surface encoded by f . Perturbing the coefficients of F gives a smooth quartic surface with similar properties.

The topology of the real surface $V_{\mathbb{R}}(F)$ is determined by the topological type of the real curve $V_{\mathbb{R}}(f)$ and its sign behavior. By perturbing F to a polynomial \tilde{F} , we can obtain a smooth quartic surface whose real part $V_{\mathbb{R}}(\tilde{F})$ has the desired topology. See [35] for details.

The construction methods in Section 4 reveal that many of the 64 types can be realized by adding a positive sextic to the product of a quartic and a conic. For such types, the sextic has the desired form $f = v_3^2 - v_2v_4$. The resulting quartic F has nice coefficients in \mathbb{Q} .

The real part of a smooth K3 surface is always an orientable surface. It has at most one connected component with nonpositive Euler characteristic — and therefore is determined (up to homeomorphism) by its total Betti number and its Euler characteristic — except when it is the union of two tori. If it is nonempty, by Smith-Thom inequality its total Betti number ranges between 2 and 24, and according to the Comessatti inequalities its Euler characteristic ranges between -18 and 20 . There are 64 possible combinations of these two numbers; they are displayed in [34, Table (3.3), page 189]. All these 64 possibilities can be realized as a quartic surface in \mathbb{P}^3 . These topological classification was studied by Utkin [35]. The isotopic and rigid isotopic classifications are due to Kharlamov [21, 22]. For proofs and further information we refer to Silhol’s book [34, Section VIII.4]. We conclude by presenting two explicit quartic surfaces that realize the minimal and the maximal Euler characteristic.

Example 6.1. Consider the smooth quartic surface $V_{\mathbb{C}}(\bar{F}) \subset \mathbb{P}^3$ defined by the polynomial

$$\begin{aligned} \bar{F} = & 100w^4 - 12500w^2x^2 + 104x^4 - 12500w^2y^2 + 1640x^2y^2 + 1550y^4 + 12500w^2yz \\ & - 75x^2yz - 1552y^3z + 9375w^2z^2 - 487x^2z^2 - 1533y^2z^2 + 354yz^3 + 314z^4. \end{aligned}$$

Its real locus $V_{\mathbb{R}}(\bar{F})$ is a connected orientable surface of genus 10. The Euler characteristic of that surface is -18 . This is the smallest possible Euler characteristic for a real K3 surface.

We constructed the quartic \bar{F} from a sextic f with ten non-nested ovals. Namely, $f = v_3^2 - v_2v_4$, where $v_4 = 33001x^4 + 131227x^2y^2 + 30980y^4 - 11842x^2yz - 62072y^3z - 155986x^2z^2 - 122652y^2z^2 + 56672yz^3 + 100672z^4$, $v_3 = 10^{-3}z^3$ and $v_2 = -4x^2 - y^2 + 2yz + 3z^2$. Our code `SexticClassifier` easily confirms that $V_{\mathbb{R}}(f)$ has Type 10. The quartic $F = v_2w^2 + 2v_3w + v_4$ has a node at $(0 : 0 : 0 : 1)$. The projection from this node is ramified at $V_{\mathbb{C}}(f)$. The K3 surface defined by $\tilde{F} = F + \epsilon w^4$ has the desired properties for $\epsilon = 10^{-10}$. Starting from \tilde{F} , we constructed \bar{F} using the techniques discussed in Section 4 for improving integer coefficients.

Our final example is dedicated to the algebraic geometer Karl Rohn, whose article [31] inspired this project. Rohn was a professor at the University of Leipzig from 1904 until 1920.

Example 6.2. We start with Rohn's imaginary symmetroid in [31, §9]. This is the quartic

$$G = \tau(s_1^2 - 6s_2)^2 + (s_1^2 - 4s_2)^2 - 64s_4,$$

where s_i is the i th elementary symmetric polynomial in x, y, z, w and $\tau = (16\sqrt{10} - 20)/135$. This is a nonnegative form with exactly 10 real zeros. Subtracting a positive definite form multiplied with a small positive scalar gives a quartic surface with ten connected components. Using the techniques in Section 4 we get the following quartic with nice integer coefficients:

$$\bar{G} = 6s_1^4 - 53s_1^2s_2 + 120s_2^2 - 320s_4.$$

The surface $V_{\mathbb{R}}(\bar{G})$ is the disjoint union of ten spheres, so it has Euler characteristic 20.

Acknowledgements. We are grateful to Paul Breiding, Claus Scheiderer, Anna Seigal, Israel Vainsencher, Emanuele Ventura and Oleg Viro for their help. This project was completed following a visit by Daniel Plaumann to MPI Leipzig. Nidhi Kaihnsa and Mahsa Sayyary Namin were funded by the International Max Planck Research School *Mathematics in the Sciences* (IMPRS). Daniel Plaumann was supported through DFG grant PL 549/3-1. Bernd Sturmfels acknowledges support by the US National Science Foundation (DMS-1419018) and the Einstein Foundation Berlin.

References

- [1] H. Abo, A. Seigal and B. Sturmfels: *Eigenconfigurations of tensors*, in Algebraic and Geometric Methods in Discrete Mathematics, (eds. H. Harrington, M. Omar and M. Wright), Contemporary Mathematics, vol **685**, American Mathematical Society (2017) 1–25.

- [2] V. I. Arnol'd: *The situation of ovals of real plane algebraic curves, the involutions of four-dimensional smooth manifolds, and the arithmetic of integral quadratic forms*, Akademija Nauk SSSR. Funkcional'nyi Analiz i ego Priloženija **5** (3) (1971), 1–9.
- [3] J. Bochnak, M. Coste and M.-F. Roy: *Real Algebraic Geometry*, Ergebnisse der Mathematik und ihrer Grenzgebiete (3), vol. 36, Springer-Verlag, Berlin, 1998.
- [4] C. Brown: *Constructing cylindrical algebraic decomposition of the plane quickly*, Manuscript, 2002.
- [5] E. Brugallé and L. López de Medrano: *Inflection points of real and tropical plane curves*, Journal of Singularities **4** (2012) 74–103.
- [6] L. Brusotti: *Sulla "piccola variazione" di una curva piana algebrica reale*, Accademia dei Lincei, Rendiconti **30** (1921) 375–379.
- [7] P. Bürgisser and F. Cucker: *Condition. The Geometry of Numerical Algorithms*, Grundlehren der Mathematischen Wissenschaften, vol. 349, Springer, Heidelberg, 2013.
- [8] J. Cheng, S. Lazard, L. Peñaranda, M. Pouget, F. Rouillier and E. Tsigaridas: *On the topology of planar curves*, Mathematics in Computer Science **4** (2010) 113–137.
- [9] S. Colley and G. Kennedy: *A higher-order contact formula for plane curves*, Comm. Algebra **19** (1991) 479–508.
- [10] W.L. Edge: *Determinantal representations of $x^4+y^4+z^4$* , Math. Proc. Cambridge Phil. Society **34** (1938) 6–21.
- [11] A. Eigenwillig, M. Kerber and N. Wolpert: *Fast and exact geometric analysis of real algebraic plane curves*, Proc. Int. Symp. Symbolic and Algebraic Computation (2007)
- [12] A. Gabard: *Ahlfors circle maps and total reality: from Riemann to Rohlin*, arXiv:1211.3680.
- [13] I.M. Gel'fand, M.M. Kapranov and A.V. Zelevinsky: *Discriminants, Resultants and Multidimensional Determinants*, Birkhäuser, Boston, 1994.
- [14] T. Fiedler: *Eine Beschränkung für die Lage von reellen ebenen algebraischen Kurven*, Beiträge zur Algebra und Geometrie **11** (1981) 7–19.
- [15] L. González-Vega and I. Necula: *Efficient topology determination of implicitly defined algebraic plane curves*, Computer Aided Geometric Design **19** (2002) 719–743.
- [16] D.A. Gudkov: *Ovals of sixth order curves*, Gor'kov. Gos.Univ.Učn.Zap.Vyp. **87** (1969) 14–20.
- [17] D. Hilbert: *Über die reellen Züge algebraischer Curven*, Math. Annalen **38** (1891) 115–138.
- [18] I.V. Itenberg: *Rigid isotopy classification of curves of degree 6 with one nondegenerate double point*, Topology of Manifolds and Varieties, Advances in Soviet Math. **18**, AMS, 1994, 193–208.
- [19] C. Kalla and C. Klein: *Computation of the topological type of a real Riemann surface*, Mathematics of Computation **83** (2014) 1823–1844.
- [20] V. M. Kharlamov: *Rigid classification up to isotopy of real plane curves of degree 5*, Funct. Anal. Appl. **15** (1981) 73–74.
- [21] V. M. Kharlamov: *Isotopic types of nonsingular surfaces of degree 4 in \mathbb{RP}^3* , Funct. Anal. Appl. **12** (1978) 86–87.
- [22] V. M. Kharlamov: *Classification of nonsingular surfaces of degree 4 in \mathbb{RP}^3 with respect to rigid isotopies*, Funct. Anal. Appl. **18** (1984) 39–45.
- [23] A. Kunert and C. Scheiderer: *Extreme positive ternary sextics*, Trans. Amer. Math. Soc., to appear.

- [24] H. Lee and B. Sturmfels: *Duality of multiple root loci*, Journal of Algebra **446** (2016) 499–526.
- [25] A. Lerario and E. Lundberg: *Statistics on Hilbert’s 16th problem*, International Mathematics Research Notices **12** (2015) 4293–4321.
- [26] M. Maccioni: *The number of real eigenvectors of a real polynomial*, arXiv:1606.04737.
- [27] M. Michalek, H. Moon, B. Sturmfels and E. Ventura: *Real rank geometry of ternary forms*, Annali di Matematica Pura ed Applicata **196** (2017) 1025–1054.
- [28] V.V. Nikulin: *Integer symmetric bilinear forms and some of their geometric applications*, USSR-Izv. **14** (1980) 103–167.
- [29] I. Petrovsky: *On the topology of real plane algebraic curves*, Ann. of Math. **39** (1938) 189–209.
- [30] D. Plaumann, B. Sturmfels and C. Vinzant: *Quartic curves and their bitangents*, Journal of Symbolic Computation **46** (2011) 712–733.
- [31] K. Rohn: *Die Maximalzahl und Anordnung der Ovale bei der ebenen Kurve 6. Ordnung und bei der Fläche 4. Ordnung*, Mathematische Annalen **73** (1913) 177–229.
- [32] V.A. Rokhlin: *Complex topological characteristics of real algebraic curves*, Russian Math. Surveys **33:5** (1978) 85–98.
- [33] R. Seidel and N. Wolpert: *On the exact computation of the topology of real algebraic curves.*, Proc 21st ACM Symposium on Computational Geometry (2005) 107–115.
- [34] R. Silhol: *Real Algebraic Surfaces*, Lecture Notes in Mathematics **1392**, Springer, Berlin, 1989.
- [35] G. A. Utkin: *Construction of certain types of nonsingular fourth order surfaces*, Gor’kov. Gos. Univ. Uën. Zap. Vyp. **87** (1969) 196–211.
- [36] N. Vervliet, O. Debals, L. Sorber, M. Van Barel and L. De Lathauwer: *Tensorlab 3.0*, Available online, March 2016, <http://www.tensorlab.net>.
- [37] O. Viro: *Gluing of plane real algebraic curves and constructions of curves of degrees 6 and 7*, In Topology (Leningrad, 1982), Lecture Notes in Math. **1060**, Springer, Berlin, 1984, 187–200.
- [38] O. Viro: *Progress in the topology of real algebraic varieties over the last six years*, Russian Math. Surveys **41** (1986) 55–82.
- [39] O. Viro: *From the sixteenth Hilbert problem to tropical geometry*, Japanese Journal of Mathematics **3** (2008) 185–214.

Authors’ addresses:

Nidhi Kaihnsa, MPI Leipzig, Nidhi.Kaihnsa@mis.mpg.de

Mario Kummer, MPI Leipzig, Mario.Kummer@mis.mpg.de

Daniel Plaumann, TU Dortmund, Daniel.Plaumann@math.tu-dortmund.de

Mahsa Sayyary Namin, MPI Leipzig, Mahsa.Sayyary@mis.mpg.de

Bernd Sturmfels, MPI Leipzig, bernd@mis.mpg.edu and UC Berkeley, bernd@berkeley.edu

Max-Planck Institute for Mathematics in the Sciences, Inselstraße 22, 04103 Leipzig, Germany

Technische Universität Dortmund, Fakultät für Mathematik, 44227 Dortmund, Germany

Department of Mathematics, University of California, Berkeley, CA 94720, USA